

Biomimetic Control of Mechanical Systems Equipped with Musculotendon Actuators

Javier Moreno-Valenzuela, Adriana Salinas-Avila

Instituto Politécnico Nacional-CITEDI, Av. del Parque 1310, Mesa de Otay, Tijuana, B.C., 22510, Mexico

Abstract

This paper addresses the problem of modelling, control, and simulation of a mechanical system actuated by an agonist-antagonist musculotendon subsystem. Contraction dynamics is given by case I of Zajac's model. Saturated semi positive proportional-derivative-type controllers with switching as neural excitation inputs are proposed. Stability theory of switched system and SOSTOOLS, which is a sum of squares optimization toolbox of Matlab, are used to determine the stability of the obtained closed-loop system. To corroborate the obtained theoretical results numerical simulations are carried out. As additional contribution, the discussed ideas are applied to the biomimetic control of a DC motor, i.e., the position control is addressed assuming the presence of musculotendon actuators. Real-experiments corroborate the expected results.

Keywords: biomimetic control, musculotendon dynamics, neural excitation, saturation, switched systems

Copyright © 2011, Jilin University. Published by Elsevier Limited and Science Press. All rights reserved.

doi: 10.1016/S1672-6529(11)60011-5

1 Introduction

To achieve the motion of body segments, such as a human leg or arm, a set of forces acting on them need to be known. These forces are produced by skeletal muscles, whose actions are individually controlled by central nervous system through neural excitation^[1].

Several mathematical models that try to define the muscle contraction properties can be found in the literature. Two very important models were proposed by Hill^[2] and Huxley^[3]. Epstein and Herzog^[4] used the biomechanical model proposed by Zajac in 1989^[1] to model the contraction dynamics. This is a Hill-type dynamical model that describes how muscle and tendon work together to produce and transmit the force to the body segments, which is referred as musculotendon model. The Zajac's model with some adaptations has been successfully used in other works to model the dynamics of mechanical systems^[5–7]. A musculoskeletal system is composed of mechanical structure (skeleton bones) and musculotendon actuators. Such system can be studied from the control theory point of view by defining inputs and outputs, so that by manipulating the input, the output is forced to be a desired one.

In a musculoskeletal system the number of muscles (inputs) is greater than the number of degrees of freedom. The simplest representation of a musculoskeletal system consists of two musculotendon actuators that interact against a common load in agonist-antagonist relationship^[6,8–10].

The position and velocity are the outputs of a musculoskeletal system, and the input is the neural excitation $u(t)$ of each muscle involved in the motion. The control problem is to design the input $u(t)$, such that the mechanical system tends to a constant desired position as time increases. Zajac's model considers that the neural excitation is presented in the set $u(t) \in [0, 1]$.

The design of controllers for mechanical system equipped with musculotendon actuators is nowadays an important topic in biomedical sciences, biomechanics and control system engineering. Next, a brief chronological literature review is provided. By using Zajac's model the musculotendon model reported in Ref. [1], Pandey *et al.*^[11] introduced an optimal control approach to find the neural control input for maximum height human jumping. Similarly, in Menegaldo's research^[7], optimal control theory was also suggested. However, unless a problem has special structures, such as the linear,

unconstrained models that produce the classic Linear-Quadratic (LQ) regulator, the evaluation and online implementation of an optimal feedback control presents a difficult challenge. The paper proposed a Proportional-Integral-Derivative (PID) controller of a bio-mechanical model^[12]. Although passive and active viscoelastic feedback from Hill-type muscle formulation is taken into account, problem of generating semi-positive control inputs for the musculotendon actuators was not unaddressed. Tahara *et al.*^[13] showed the modelling and control of a kind of musculoskeletal system, where the muscle model is based on Hill's model. The control system consisted in generating semi-positive activation levels to stabilize the position. Moody *et al.*^[14] proposed an elasto-dynamic model of the human arm that includes effects of neuro-muscular control upon elastic deformation in the limb. Muscle forces derived from a Hill-type model of musculotendon dynamics are assumed. To control the arm motion, neural feedback and feedforward control is proposed. Laczko *et al.*^[15] took a different approach which specifically introduced muscle activity patterns for generating desired angular changes in the human arm and in the lower limb.

As shown in the literature review, a few works have presented a solution for the stabilization problem of mechanical systems actuated by musculotendon actuators taking into account the saturated semi positive constraint of the neural excitation $u(t) \in [0, 1]$.

To the best of the authors' knowledge, the idea that the control input $u(t) \in [0, 1]$ can be designed by using a new switched control systems approach. Specifically, in this paper, saturated semi positive control inputs are generated by a commutation control law, which converts the closed-loop system into a switched system that belongs to the class called hybrid systems. Since many of the systems encountered in practice are of hybrid nature, in the last few years, this kind of systems have been an interdisciplinary and very active area of research^[16]. Hybrid system theory facilitates the study of complex systems by decomposing them into simpler systems and by allowing the use of well-known control tools as Lyapunov theory.

The stability of a switched system under arbitrary switching can be achieved by finding a single Lyapunov function whose derivative along solutions of all subsystems satisfies the inequalities of the Lyapunov's direct method. Such function is called common Lyapunov

function^[16-18]. Due to the high order and nonlinearity of the systems studied here, it is extremely difficult to find a common Lyapunov function in a generalized way. To find a numerical solution, SOSTOOLS is used, which is a free MATLAB toolbox for formulating and solving sums of squares optimization programs^[18-20].

On the other hand, researchers are looking in cupboards and under rocks for biological inspiration to create a new generation of flying, crawling, and swimming automats known as biomimetic robots. It has been expected that the robots will be able to cwork and coexist with a human at home or a workspace in the near future. However, no matter how similar to a human being in appearance the robot is, it is very difficult to cwork with a human in daily activities if it cannot act or perform a task with human-like movements. Hence the importance of the development of control strategies is to obtain biomimetic behavior of the mechanical system, which has particular applications in humanoids robots.

The main contributions of the study presented in this paper are: (1) The modelling of a biomechanical systems where musculotendon actuators are used; (2) A new control law based on switched system theory, which guarantees that the produced control action is semi positive; (3) The application of the proposed ideas in the biomimetic control of a DC motor^[21]. In this respect, the position control of the motor shaft is addressed assuming the presence of musculotendon actuators. Real-time experiments corroborate the expected results.

This paper is organized as follows. Section 2 describes the biomechanical model to be controlled. In section 3, the results related to the saturated control of the derived biomechanical system are given. In section 4, the proposed switched control law is applied to the control of a DC motor assuming that it is actuated by musculotendons. Real-time experiments are also described. Finally, concluding remarks are drawn in section 5.

2 Development of the biomechanical model and control goal

In this section we present the derivation of a biomechanical model and the equations of the model. Then the equations for the activation and musculotendon contraction subsystems are provided. The formulation of the control objective is also introduced.

2.1 Mechanical subsystem

The dynamics of the mechanical subsystem, as shown in Fig. 1, is given by

$$M\ddot{x}_1 + F_v\dot{x}_1 = F_1^T - F_2^T, \quad (1)$$

where M (kg) is the mass of mechanical subsystem, F_v ($\text{kg}\cdot\text{m}\cdot\text{s}^{-1}$) is the viscosity, $x_1 = L_1^{\text{MT}}$ (m) is the length of actuator 1, is the velocity of actuator 1, F_1^T (N) is the force developed by actuator 1 and F_2^T (N) is the force developed by actuator 2. Let us notice that in the agonist-antagonist relationship, the net force that acts on the load is given by $F_1^T - F_2^T$ (see for example Ref. [8]).

Let us consider the system described in Fig. 1. This case study considers that $L = \text{constant}$, i.e., one muscle lengthens as the agonist while the other contracts as the antagonist. In this way, the relationship between lengths L_1^{MT} and L_2^{MT} and velocities V_1^{MT} , and V_2^{MT} is obtained.

Specifically, the length of actuator 1 is given by $x_1 = L_1^{\text{MT}}$, then, in consideration of Fig. 1, the length of actuator 2 is

$$x_1 = L - x_1', \quad (2)$$

where L is distance between the points of attaching of one actuator to the another. Being $x_d > 0$ the desired position of the mass, it is possible to define the desired position of the mass with respect to the origin of actuator 2 as

$$x_d' = L - x_d. \quad (3)$$

Using Eq. (2), the position error is defined as

$$\tilde{x}_1 = x_d - x_1 = x_d - L_1^{\text{MT}}, \quad (4)$$

where $0 < x_d < L$ is the desired position of the mass with respect to the origin of actuator 1 and x_1 is the position of the mass. The position error with respect to actuator 2 can be computed as $\tilde{x}_1' = x_d' - x_1' = -x_d + x_1 = -\tilde{x}_1$. As expected, the position errors \tilde{x}_1 and \tilde{x}_1' have opposite signs.

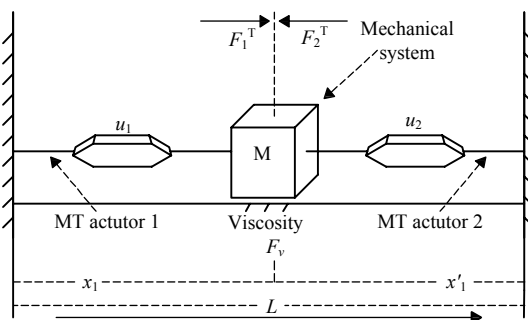


Fig. 1 Agonist-antagonist muscletendon pair acting on a common mass-damper system.

2.2 Zajac's model

In this model, the input $u(t)$ is the net neural input to the muscle, and the output $F^T(t)$ is the tendon force (see Fig. 2).

The force $F^T(t)$ developed by the actuator depends on the velocity $V^{\text{MT}}(t)$ and the length $L^{\text{MT}}(t)$, which are determined from the position of the body segments (mechanical system). At the same time, the dynamics of the body segments depends on the force $F^T(t)$ developed by the muscletendon actuator. The dynamics of the muscletendon actuator is composed of activation dynamics and muscletendon contraction dynamics (see Fig. 2). In the original work, Zajac presented the obtained model in normalized quantities with the optimal muscle length L_0^M , the maximum shortening velocity V_m and the maximum active force F_0^M produced by the muscle in an isometric contraction.

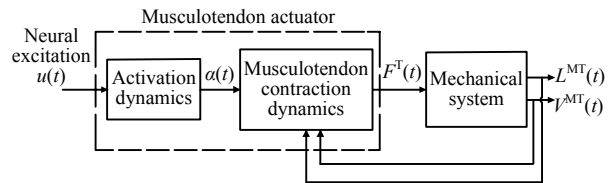


Fig. 2 Block diagram that shows the interaction of tendon and muscle with a mechanical system.

2.3 Activation dynamics subsystem

The activation in the muscletendon model is a variable that affects only the muscle and is given as

$$\frac{da(t)}{dt} + \left[\frac{1}{\tau_{\text{act}}} [\beta + [1 - \beta]u(t)] \right] a(t) = \frac{1}{\tau_{\text{act}}} u(t), \quad (5)$$

where $a(t)$ is the muscle activation, with constraint $0 \leq a(t) \leq 1$. The value $a(t) = 1$ indicates that the muscle is fully activated, and $a(t) = 0$ fully deactivated. $u(t)$ is the neural excitation, which denotes the control input, with constraint $0 \leq u(t) \leq 1$. τ_{act} is the time constant when muscle is fully excited ($u(t) = 1$). $\beta \equiv \tau_{\text{act}}/\tau_{\text{dact}}$, where τ_{dact} is the time constant when muscle is fully deactivated ($u(t) = 0$), $0 < \beta < 1$.

An examination of the term in the brackets shows that when the muscle is fully activated, i.e., $u(t) = 1$, the time constant of $a(t)$ is given by τ_{act} . However, when the muscle is fully deactivated, i.e., when $u(t) = 0$, the time constant is τ_{act}/β . One consequence of this model is that active isometric force rises faster during excitation than it falls during relaxation, a property that has been well studied^[2,22].

2.4 Musculotendon contraction dynamics subsystem

The essential part of the Zajac's model is the force dynamics, also named musculotendon contraction dynamics. Musculotendon contraction represents the integrated dynamical process of muscle and tendon working together^[1].

By assuming that the line of action of the muscle fibers is parallel to the line of action of the tendon, the musculotendon contraction dynamics is written in its normalized form as

$$\frac{d\tilde{F}^T}{d\tau} = \tilde{k}^T [\tilde{V}^{MT} - \tilde{V}^M(\tilde{L}^M, \tilde{F}^T, a(\tau))], \quad (6)$$

where
$$\tilde{F}^T = \frac{F^T}{F_0^M} = \tilde{F}^M, \quad (7)$$

with F_0^M the peak isometric active force, is the normalized tendon force which is equal to the normalized muscle force,

$$\tau = \left(\frac{1}{\tau_c}\right)t \quad (8)$$

is the normalized time,

$$\tilde{k}^T = k^T \left(\frac{L_0^M}{F_0^M}\right) \quad (9)$$

is the normalized tendon stiffness,

$$\tilde{V}^{MT} = V^{MT} \left(\frac{1}{V_m}\right) \quad (10)$$

is the normalized MT velocity, and

$$\tilde{V}^M = f(\tilde{L}^M, \tilde{F}^T, a(\tau)) \quad (11)$$

is the normalized muscle velocity for a given fiber length, muscle force and activation level (called Force-Velocity-Length relationship (FVL) of a Hill-type model).

2.5 Case I: Flat region of the force-length curve

The case I presented in Ref. [1] is the model of the contraction dynamics Eq. (6) when the muscle operates at the flat region of its force-length curve. Thus, the linear relationship FVL is given by

$$-\tilde{V}^M = a(\tau) - \tilde{F}^M, \quad (12)$$

where $a(\tau)$ is the activation level as a function of the normalized time τ .

The musculotendon contraction dynamics of case I is obtained by replacement of Eq. (12) in Eq. (6)

$$\frac{d\tilde{F}^T}{d\tau} + \tilde{k}^T \tilde{F}^T = \tilde{k}^T [\tilde{V}^{MT} + a(\tau)]. \quad (13)$$

Eq. (13) is normalized with L_0^M , F_0^M and V_m . To work with dimensional quantities, by using the definitions of Eqs. (7)–(11), and take into account that the linear approximation for \tilde{k}^T in Eq. (13), which was defined in Ref. [1] as $\tilde{k}^T = 30 L_0^M / L_s^T$, where L_s^T is the tendon slack length, then Eq. (13) is rewritten as

$$\frac{dF^T}{dt} = -\frac{30V_m}{L_s^T} F^T + \frac{30F_0^M}{L_s^T} V^{MT} + \frac{30F_0^M V_m}{L_s^T} a(t), \quad (14)$$

where F^T is the musculotendon actuator force, $a(t)$ is the activation level defined in Eq. (5).

2.6 State variables of the overall biomechanical system

By using Eqs. (1), (4), (5) and (14), the open-loop system can be written as

$$\frac{d}{dt} \begin{bmatrix} \tilde{x}_1 \\ x_2 \\ x_3 \\ x_4 \\ x_5 \\ x_6 \end{bmatrix} = \begin{bmatrix} -x_2 \\ \frac{1}{M} [x_3 - x_4 - F_v x_2] \\ \frac{30F_{01}^M}{L_{s1}^T} x_2 + \frac{30F_{01}^M}{L_{s1}^T} x_5 - \frac{30V_{m1}}{L_{s1}^T} x_3 \\ -\frac{30F_{02}^M}{L_{s2}^T} x_2 + \frac{30F_{02}^M}{L_{s2}^T} x_6 - \frac{30V_{m2}}{L_{s2}^T} x_4 \\ [c_{31} - c_{21} x_5] u_1(t) - c_{11} x_5 \\ [c_{32} - c_{22} x_6] u_2(t) - c_{12} x_6 \end{bmatrix}, \quad (15)$$

where $x_2 = \dot{x}_1$, $\beta_p = \tau_{actp} / \tau_{dactp}$, $x_3 = F_1^T$, $c_{1p} = \beta_p / t_{actp}$, $x_4 = F_2^T$, $c_{2p} = (1 - \beta_p) / t_{actp}$, $x_5 = a_1(t)$, $c_{3p} = 1 / t_{actp}$, $x_6 = a_2(t)$, with $p = 1, 2$.

2.7 Control objective

Considering the biomechanical system Eq. (15), the control problem revolves around the design of constrained neural control inputs

$$u_1(t), u_2(t) \in [0, 1], \quad (16)$$

such that for some bounded set of initial conditions $[\tilde{x}_1(0)x_2(0)x_3(0)x_4(0)x_5(0)x_6(0)]^T \in \mathbf{R}_a$, the limit

$$\lim_{t \rightarrow \infty} \tilde{x}_1(t) = 0 \quad (17)$$

is satisfied, where \tilde{x}_1 denotes the position error, which was defined in Eq. (4). The set \mathbf{R}_a is defined as the domain of attraction of the system Eq. (15). In other words, the set \mathbf{R}_a is such that the limit of every trajectory of

Eq. (15) starting in R_a is the equilibrium point. For the sake of shortening, the computation of the domain of attraction is not considered in this paper.

3 Control of the biomechanical model

The control of the biomechanical system Eq. (15) is studied in this section. In order to introduce the proposed controller, some mathematical preliminaries on switched systems are provided. Then, the control laws u_1, u_2 , to satisfy the control objective Eq. (17) are introduced. The stability of the resulting closed-loop system and numerical results are discussed also.

3.1 Stability of switched systems

Systems that have dynamics that are described by a set of continuous time differential equations in conjunction with a discrete event process are usually referred to as switched or hybrid systems. Such systems are of the form:

$$\dot{\mathbf{x}} = \mathbf{f}_i(\mathbf{x}), i \in \mathbf{I} = \{1, \dots, N\}, \quad (18)$$

where $\mathbf{x} \in \mathbb{R}^n$ is the continuous state, N is the number of components of the family of vector field $\mathbf{f}_i(\mathbf{x})$, i is the discrete state, $\mathbf{f}_i(\mathbf{x})$ is the vector field describing the dynamics of the i th mode/subsystem, and \mathbf{I} is the index set. The difference between switched and hybrid systems is that in the former only one $i \in \mathbf{I}$ is possible for each $\mathbf{x} \in \mathbb{R}^n$, and in the later multiple i are possible for some $\mathbf{x} \in \mathbb{R}^n$. Without loss of generality, we assume that the state space origin $\mathbf{x} = 0 \in \mathbb{R}^n$ is an equilibrium point^[18].

This study focuses on switched systems, where switching events can be classified into state-dependent or time-dependent (see Ref. [16]).

According to switched systems theory, local stability of system Eq. (18) under arbitrary switching can be studied using the following theorems:

Theorem 1: [Theorem 1 in Ref. [18]] Suppose that for the set of vector fields $\{\mathbf{f}_i(\mathbf{x})\}$ there exists a polynomial $V(\mathbf{x})$ such that $V(0) = 0$ and

$$V(\mathbf{x}) > 0 \quad \forall \mathbf{x} \neq 0, \quad (19)$$

$$\frac{\partial V}{\partial \mathbf{x}} \mathbf{f}_i(\mathbf{x}) < 0 \quad \forall \mathbf{x} \neq 0, i \in \mathbf{I}. \quad (20)$$

Then the origin of the state space of the system Eq. (18) is globally asymptotically stable under arbitrary switching.

Theorem 2: [Theorem 1 in Ref. [17]] If the differential equations corresponding to the linearization of

system Eq. (18) are (asymptotically) stable in x_0 and have the same quadratic Lyapunov function, then the system Eq. (18) is (asymptotically) stable in x_0 .

3.2 Switching control law for the controllers $u_1(t)$ and $u_2(t)$

In this section we explain how our solution satisfies the condition Eq. (16) and accomplishes the control objective Eq. (17). Let us recall the well-known Proportional-Derivative (*PD*) controller:

$$PD = k_p \tilde{x}_1 - k_v x_2, \quad (21)$$

where \tilde{x}_1 is the position error of the mass, x_2 is the velocity and $k_p, k_v > 0$.

In order to satisfy the constraint Eq. (16) in $u_1(t)$ and $u_2(t)$, the *PD* controller Eq.(21) can be used in the switching control law:

$$u_1(t) = \begin{cases} \tanh(\mu_1 PD) & \text{if } PD \geq 0, \\ 0 & \text{if } PD < 0, \end{cases} \quad (22)$$

where $u_1(t) \in [0, 1]$ is the input for actuator 1, and $\mu_1 > 0$, and

$$u_2(t) = \begin{cases} 0 & \text{if } PD < 0, \\ -\tanh(\mu_2 PD) & \text{if } PD \geq 0, \end{cases} \quad (23)$$

where $u_2(t) \in [0, 1]$ is the input for the actuator 1, and $\mu_2 > 0$.

The switching between the control inputs depends on the sign of *PD* controller Eq. (21), which in turn depends on the state variables \tilde{x}_1 and x_2 . Thus, Eqs. (22) and (23) define a switched control law, which accomplishes the constraint Eq. (16), for the system Eq. (15).

3.3 Feedback control system

With the control inputs Eqs. (22) and (23) the open-loop system Eq. (15) turns into two feedback subsystems $\mathbf{f}_1(\mathbf{x})$ and $\mathbf{f}_2(\mathbf{x})$, which commute by the switching law:

$$\dot{\mathbf{x}} = \mathbf{f}(\mathbf{x}) = \begin{cases} \mathbf{f}_1(\mathbf{x}) & \text{if } PD \geq 0, \\ \mathbf{f}_2(\mathbf{x}) & \text{if } PD < 0. \end{cases} \quad (24)$$

System Eq. (24) operates in the subsystem $\mathbf{f}_1(\mathbf{x})$ for nonnegative values of *PD* (with $u_1(t) \in [0, 1]$ and $u_2(t) = 0$), and operates in the subsystem $\mathbf{f}_2(\mathbf{x})$ for negative values of *PD* (with $u_1(t) = 0$ and $u_2(t) \in [0, 1]$). Fig. 3 shows a block diagram of the system Eq. (24).

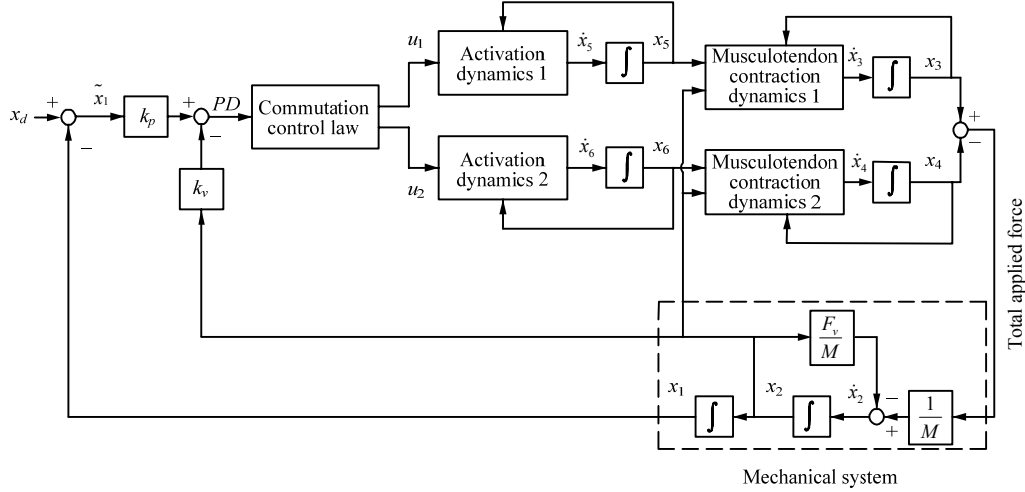


Fig. 3 Block diagram that represents the feedback control system Eq. (24).

Given the control inputs $u_1(t)$ and $u_2(t)$, the obtained feedback system Eq. (24) is a state-dependent switched system, where switching depends on the state variables \tilde{x}_1 and x_2 . In other words, the system Eq. (24) has the form of Eq. (18), with $i \in I = \{1, 2\}$, i.e., the system consists of two operating regions: region 1 if $PD \geq 0$, and region 2 if $PD < 0$.

According to Theorems 1 and 2, the state space origin $\mathbf{x} = 0 \in \mathbb{R}^n$ of the nonlinear system Eq. (24) is a locally (asymptotically) stable equilibrium point if the linearized system is (asymptotically) stable.

The state space origin $\mathbf{x} = 0 \in \mathbb{R}^n$ is a common equilibrium point of the subsystems $\mathbf{f}_1(\mathbf{x})$ and $\mathbf{f}_2(\mathbf{x})$. By linearizing the system Eq. (24) around $\mathbf{x} = 0 \in \mathbb{R}^n$, we obtain the following switched system:

$$\dot{\mathbf{x}} = \begin{cases} \mathbf{A}_1 \mathbf{x} & \text{if } PD \geq 0, \\ \mathbf{A}_2 \mathbf{x} & \text{if } PD < 0, \end{cases} \quad (25)$$

where PD is given in Eq. (21), and

$$\mathbf{A}_1 = \begin{bmatrix} 0 & a_{12} & 0 & 0 & 0 & 0 \\ 0 & a_{22} & a_{23} & a_{24} & 0 & 0 \\ 0 & a_{32} & a_{33} & 0 & a_{35} & 0 \\ 0 & a_{42} & 0 & a_{44} & 0 & a_{46} \\ a_{51} & a_{52} & 0 & 0 & a_{55} & 0 \\ 0 & 0 & 0 & 0 & 0 & a_{66} \end{bmatrix},$$

$$\mathbf{A}_2 = \begin{bmatrix} 0 & b_{12} & 0 & 0 & 0 & 0 \\ 0 & b_{22} & b_{23} & b_{24} & 0 & 0 \\ 0 & b_{32} & b_{33} & 0 & b_{35} & 0 \\ 0 & b_{42} & 0 & b_{44} & 0 & b_{46} \\ 0 & 0 & 0 & 0 & b_{55} & 0 \\ b_{61} & b_{62} & 0 & 0 & 0 & b_{66} \end{bmatrix},$$

where $a_{12} = -1$, $a_{22} = -Fv/M$, $a_{23} = 1/M$, $a_{24} = -1/M$, $a_{32} = 30F_{01}^M / L_{s1}^T$, $a_{33} = -30V_{m1} / L_{s1}^T$, $a_{35} = 30F_{01}^M V_{m1} / L_{s1}^T$, $a_{42} = -30F_{02}^M / L_{s2}^T$, $a_{44} = -30V_{m2} / L_{s2}^T$, $a_{51} = c_{31}k_p$, $a_{46} = 30F_{02}^M V_{m2} / L_{s2}^T$, $a_{52} = -c_{31}k_v$, $a_{55} = -c_{11}$, $a_{66} = -c_{12}$; $b_{12} = -1$, $b_{22} = -Fv/M$, $b_{23} = 1/M$, $b_{24} = -1/M$, $b_{32} = 30F_{01}^M / L_{s1}^T$, $b_{33} = -30V_{m1} / L_{s1}^T$, $b_{35} = 30F_{01}^M V_{m1} / L_{s1}^T$, $b_{42} = -30F_{02}^M / L_{s2}^T$, $b_{44} = -30V_{m2} / L_{s2}^T$, $b_{46} = 30F_{02}^M V_{m2} / L_{s2}^T$, $b_{55} = -c_{11}$, $b_{61} = -c_{32}k_p$, $b_{62} = c_{32}k_v$, $b_{66} = -c_{12}$.

The problem is to find a common Lyapunov function $V(\mathbf{x})$ that satisfies the conditions Eqs. (19) and (20) for the linearized system Eq. (25). A numeric common Lyapunov function is obtained with the purpose of proving that the system Eq. (25) is asymptotically stable.

3.3.1 Numerical case study

First, let us notice that a necessary condition for (asymptotic) stability under arbitrary switching is that all of the individual subsystems are (asymptotically) stable [23]. Thus, using the root locus of the characteristic equation of each subsystem

$$\dot{\mathbf{x}} = \mathbf{A}_i \mathbf{x}, i = 1, 2.$$

We have computed numerical values of μ_1, μ_2 , k_p and k_v such that \mathbf{A}_i , $i = 1, 2$, are Hurwitz.

The roots of a characteristic equation are obtained by solving

$$\det[\lambda \mathbf{I}_6 - \mathbf{A}_i] = 0. \quad (26)$$

The linear subsystem $\dot{\mathbf{x}} = \mathbf{A}_i \mathbf{x}$ is asymptotically stable if

$$\Re(\lambda_j \{\mathbf{A}_i\}) < 0 \quad \forall j = \{1, 2, \dots, 6\}, i \in I = \{1, 2\}. \quad (27)$$

To prove the effectiveness of the proposed control law, a

numerical case is presented. For such purpose, identical actuators are considered. The numerical parameters L_0^M , L_s^M and F_0^M of the brachioradialis muscle presented in Ref. [24] are used. The values for τ_c , τ_{act} and τ_{dact} are taken from Ref. [1]: $L_{0p}^M=0.2703$ cm, $\tau_c=0.1$ s, $F_{0p}^M=101.58$ N, $\tau_{actp}=0.015$ s, $L_{sp}^T=0.0604$ cm, $\tau_{dactp}=0.050$ s, where $p=1,2$. Mass M and viscosity F_v are proposed as: $M=3.8$ kg, $F_v=1$ kg·m·s⁻¹. With the root locus of the individual characteristic equations in Eq.(26), we propose the parameters μ_1, μ_2, k_p and k_v for the control inputs $u_1(t)$ and $u_2(t)$: $\mu_1=1$, $k_p=0.003$, $\mu_2=1$, $k_v=0.23$. The proposed parameters μ_1, μ_2, k_p and k_v , allow us to satisfy the local stability condition Eq. (27). Small values of the mass and the viscosity can be used in the musculotendon actuators by using small values of parameter F_0^M .

3.3.2 Using SOSTOOLS to find a common Lyapunov function

Once obtained the stability conditions for the individual subsystems $\dot{x} = A_i x$ ($i=1, 2$) of Eq. (25), a common Lyapunov function $V(x)$ that satisfies the inequalities Eqs. (19) and (20) is constructed. Such a function is obtained by using SOSTOOLS^[20] and can be written as follows:

$$V(x) = x^T P x, \quad x \in \mathbb{R}^6, \quad P = P^T > 0, \quad P \in \mathbb{R}^{6 \times 6}, \quad (28)$$

$$\text{and} \quad P = \begin{bmatrix} p_{11} & p_{12} & p_{13} & p_{14} & p_{15} & p_{16} \\ p_{21} & p_{22} & p_{23} & p_{24} & p_{25} & p_{26} \\ p_{31} & p_{32} & p_{33} & p_{34} & p_{35} & p_{36} \\ p_{41} & p_{42} & p_{43} & p_{44} & p_{45} & p_{46} \\ p_{51} & p_{52} & p_{53} & p_{54} & p_{55} & p_{56} \\ p_{61} & p_{62} & p_{63} & p_{64} & p_{65} & p_{66} \end{bmatrix}, \quad (29)$$

where $p_{11} = 0.20831$, $p_{12} = p_{21} = -0.21327$, $p_{13} = p_{31} = -0.42936 \times 10^{-4}$, $p_{14} = p_{41} = 0.42936 \times 10^{-4}$, $p_{15} = p_{51} = p_{16} = p_{61} = -0.28448$, $p_{22} = 0.46856$, $p_{23} = p_{32} = 0.09139 \times 10^{-3}$, $p_{33} = p_{44} = 0.58872 \times 10^{-7}$, $p_{24} = p_{42} = -0.09139 \times 10^{-3}$, $p_{34} = p_{43} = -0.22359 \times 10^{-7}$, $p_{25} = p_{52} = 0.6145$, $p_{26} = p_{62} = -0.6145$, $p_{35} = p_{53} = p_{46} = p_{64} = 0.11783 \times 10^{-3}$, $p_{36} = p_{63} = p_{45} = p_{54} = -0.12188 \times 10^{-3}$, $p_{55} = p_{66} = 0.82876$, $p_{56} = p_{65} = -0.8258$.

The common Lyapunov function Eq. (28), with P in Eq. (29), leads to the conclusion that, by Theorem 1, the state space origin $x = 0 \in \mathbb{R}^6$ of the the switched system Eq. (25) is asymptotically stable. Therefore, according to Theorem 2, the state space origin $x = 0 \in \mathbb{R}^6$ of the system Eq. (24) is locally asymptotically stable.

3.4 Results and discussions

With the obtained local stability of the system Eq.(24), a simulation using Matlab is presented. In this simulation the system initial conditions are equal to zero, except for the position error, which starts with a value of $\tilde{x}_1(0) = 0.05$ m. With these initial conditions the system starts in the region 1.

Fig. 4 shows the position error $\tilde{x}_1(t)$. The saturated control inputs $u_1(t)$ and $u_2(t) \in [0,1]$ are shown in Fig. 5. The graph to compare the function $V(x)$ evaluated along the systems Eq. (24) (dashed line) and Eq. (25) (continuous line) is presented in Fig. 6. In this figure, vertical lines indicate the switching between regions 1 and 2 for the systems Eq. (24) (dashed line) and Eq. (25) (continuous line).

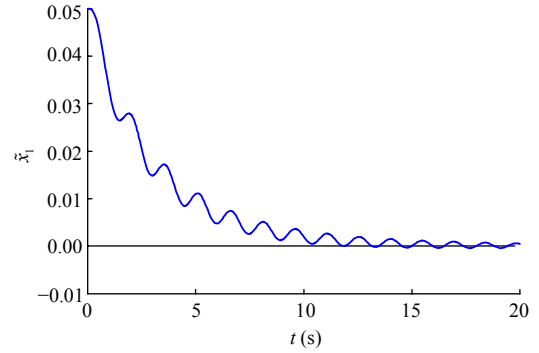


Fig. 4 Position error $\tilde{x}_1(t)$.

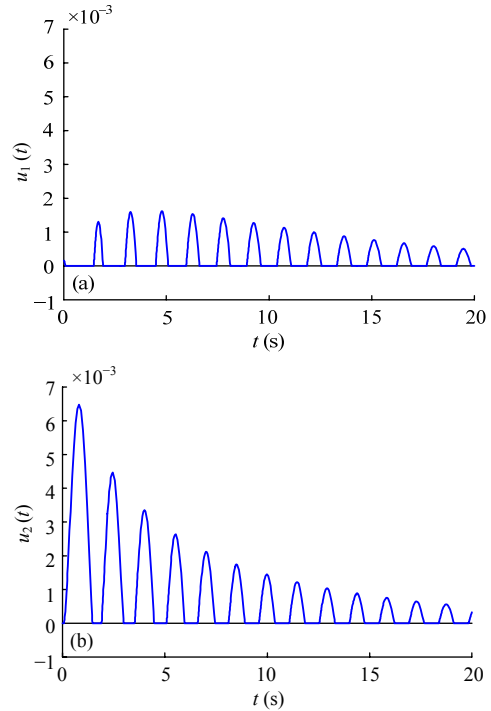


Fig. 5 Time history of the musculotendon control inputs $u_1(t)$ and $u_2(t)$.

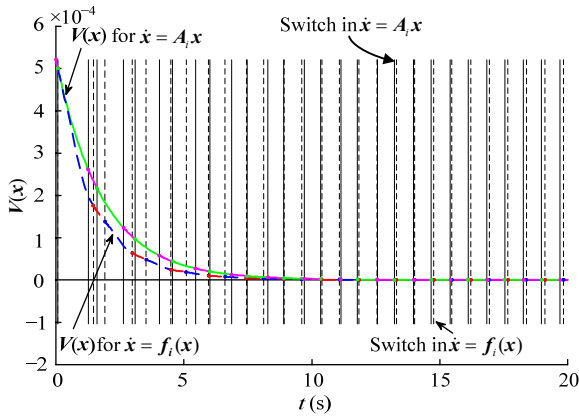


Fig. 6 Common Lyapunov function $V(x)$.

It is worthwhile to notice that several sets of control parameters μ_1 , μ_2 , k_p and k_v , that rendered the closed-loop system Eqs. (15) – (23) locally asymptotically stable were found. For each one of those sets of control parameters, a common Lyapunov function was obtained, while the necessary condition of Hurwitz matrices A_1 and A_2 was also achieved.

With respect to the present example, which considered two identical musculotendon actuators, the following observations on the tuning of control gains k_p and k_v are in order: (1) Numerical value in the gain k_p is lower than the one used to produce a reduction in the oscillations of the error position $\tilde{x}_1(t)$, i.e., the closed-loop system Eqs. (15) – (23) become “more stable”. (2) However, although a smoothed response is obtained, the reduction of k_p increases the settling time. (3) With a larger numerical value of k_p , oscillations of the error position $\tilde{x}_1(t)$ are increased and even instability is observed. (4) For a fixed k_p , increasing the gain k_v seems to make the system more stable since the roots of the characteristic equation of A_1 and A_2 move to the left half-plane of the complex plane. The opposite effect is observed with reduction of k_v .

Although some insight in the tuning of the control parameters μ_1 , μ_2 , k_p and k_v , has been obtained, actually we are trying to obtain an analytic method to find explicit tuning bounds on those parameters.

For this numerical case study, the numerical values of the control inputs $u_1(t)$ and $u_2(t)$ are small, as seen in Fig. 5. However, if there is a large position error $\tilde{x}_1(t)$, then large forces will be required in the musculotendon actuators, which, at the same time, will imply the application of large neural excitation inputs $u_1(t)$ and $u_2(t)$.

However, thanks to the incorporation of the hyperbolic tangent function in the switched controller Eqs. (22) – (23), no matter how large is the position error $\tilde{x}_1(t)$, the neural excitation inputs $u_1(t)$ and $u_2(t)$ will be evaluated into the set $[0,1]$.

The studied biomechanical system Eq. (15) can be seen as a simplified model of a human arm. Since the parameters of the actuators are assumed to match the behavior of real human muscles^[24], one would expect that the performed motion is smooth as done by a real human arm. However, the simulation shows that the performed motion presents oscillations that vanish asymptotically as time increasing. Let us notice that a response without oscillations could be obtained by changing the selected parameters of the controller, in particular, by increasing the value of k_v , which at the same time increases the damping of the overall closed-loop system. In the presented numerical study the selection of the values of the controller gains and the musculotendon actuator parameters is intended to show the ability of the control law to regulate the position of the biomechanical system by turning on and turning off the neural inputs. Besides, the numerical value of the mass M and the viscous friction coefficient F_v is not necessarily related to the physics of an human arm. Analogy of the proposed switched control law with real-time response of a human arm requires further study.

An important issue is the co-contraction, which is defined as simultaneous activation of antagonistic muscles crossing a joint. Its purpose is to augment the ligament function in maintenance of joint stability, provide resistance to rotation at a joint, and equalize the pressure distribution at the articular surface^[25,26]. In other words, muscle co-contraction is defined as the simultaneous activation of antagonist and agonist muscle groups of the same joint and in the same plane of movement. As seen in Fig. 7, both musculotendon actuators deliver force at the same time, whereby co-contraction is introduced by the proposed control scheme. The reason for the presence of co-contraction is that the muscle activation levels $a_1(t)$, $a_2(t)$ are kept positive during the time that one neural input has some non negative value and another is null. Thus, the activation and contraction dynamics work as memory of the overall musculotendon actuator.

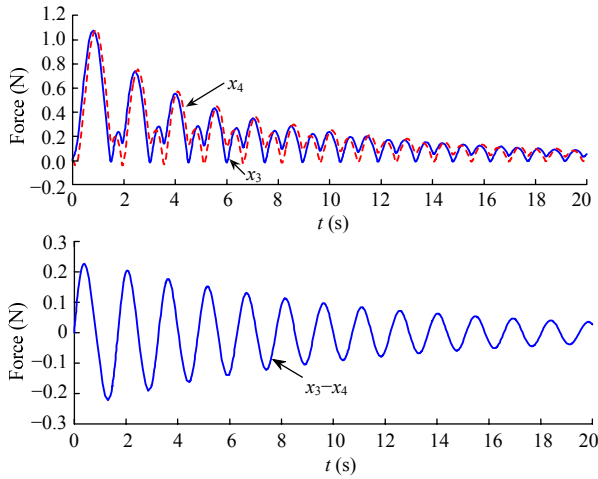


Fig. 7 Time history of the force delivered by each musculotendon actuator $x_3(t)$, $x_4(t)$, and the total force applied to the body $F^T(t) = x_3(t) - x_4(t)$.

4 Application for the biomimetic control of a DC motor

As pointed out in Ref. [27], remarkable developments of human-shaped robots have been achieved with the latest progress of robotic technology in recent years^[28,29], so that friendly feeling of human toward the robot is practically realized from a cosmetic point of view.

The interest in studying muscle-tendon models that interact with mechanical systems as well as their control is to achieve applications in mechatronics and robotics where a biomimetic like behavior is important. Let us notice that robot models interconnected with muscle-tendon systems have characteristics of human movements, which is important to generate a human-like behavior when controlling the humanoid robots. A recent survey on biomimetic planning and controlling of mechanical system can be found in Ref. [21].

Specifically, the final goal of this section is to control a single second order mechanical system (a linear DC motor system) with human-like movement. The biomimetic behavior is obtained by considering that the motor model is actuated by an agonist-antagonist muscle-tendon subsystem. The two neural control inputs are generated by the proposed commutation control law of Eqs. (22) and (23). Simulations and experiments show the viability of the proposed theory.

4.1 Motor system and generalization of the musculotendon dynamics

Let us consider the DC motor model

$$J\ddot{x}(t) + F_v\dot{x}(t) = \bar{k}v(t), \quad (30)$$

where x denotes the rotor position, J is rotor inertia, F_v is the viscous friction coefficient, and \bar{k} is the voltage to torque conversion factor. The voltage input $v(t)$ is generated through $F_1^T(t)$ and $F_2^T(t)$, i.e., the outputs of two musculotendon actuators implemented by software. Specifically,

$$v(t) = F_1^T(t) - F_2^T(t). \quad (31)$$

The overall model (the DC motor and the musculotendon actuators) can be written in state variables as

$$\mathbf{f}(x) = \frac{d}{dt} \begin{bmatrix} \tilde{x}_1 \\ x_2 \\ x_3 \\ x_4 \\ x_5 \\ x_6 \end{bmatrix} = \begin{bmatrix} -x_2 \\ -\frac{F_v}{J}x_2 + \frac{\bar{k}}{J}[x_3 - x_4] \\ \frac{30F_{01}^M}{L_{s1}^T}x_2 + \frac{30F_{01}^M V_{m1}}{L_{s1}^T}x_5 - \frac{30V_{m1}}{L_{s1}^T}x_3 \\ -\frac{30F_{02}^M}{L_{s2}^T}x_2 + \frac{30F_{02}^M V_{m2}}{L_{s2}^T}x_6 - \frac{30V_{m2}}{L_{s2}^T}x_4 \\ [c_{31} - c_{21}x_5]u_1(t) - c_{11}x_5 \\ [c_{32} - c_{22}x_6]u_2(t) - c_{12}x_6 \end{bmatrix}. \quad (32)$$

Considering that the musculotendon actuators 1 and 2 are identical, it is possible to generalize the open-loop model Eq. (32) as

$$\mathbf{f}(x) = \frac{d}{dt} \begin{bmatrix} \tilde{x}_1 \\ x_2 \\ x_3 \\ x_4 \\ x_5 \\ x_6 \end{bmatrix} = \begin{bmatrix} -x_2 \\ -\frac{F_v}{J}x_2 + \frac{\bar{k}}{J}[x_3 - x_4] \\ -k_1x_3 + k_2x_2 + k_3x_5 \\ -k_1x_4 - k_2x_2 + k_3x_6 \\ [c_3 - c_2x_5]u_1(t) - c_1x_5 \\ [c_3 - c_2x_6]u_2(t) - c_1x_6 \end{bmatrix}. \quad (33)$$

Note that the musculotendon constants k_1 , k_2 , k_3 , c_1 , c_2 , and c_3 are interpreted as parameters that govern the time evolution of the biomimetic controller Eq. (31).

4.2 Switched control law

To stabilize the position error $\tilde{x}_1(t)$ we have used the switched control law Eqs. (22) and (23). Substituting Eqs. (22) and (23) in the open-loop system Eq. (33), we obtain a switched system with structure

$$\dot{x} = \mathbf{f}(x) = \begin{cases} \mathbf{f}_1(x), & \text{if } PD \geq 0, \\ \mathbf{f}_2(x), & \text{if } PD < 0. \end{cases} \quad (34)$$

Following the ideas in the section 3, the problem is to find a common Lyapunov function $V(x)$ for the linearization of the subsystems Eq. (34), which is given by

$$\dot{\mathbf{x}} = \begin{cases} \mathbf{A}_1 \mathbf{x}, & \text{if } PD \geq 0, \\ \mathbf{A}_2 \mathbf{x}, & \text{if } PD < 0, \end{cases} \quad (35)$$

where

$$\mathbf{A}_1 = \begin{bmatrix} 0 & -1 & 0 & 0 & 0 & 0 \\ 0 & -\frac{F_v}{J} & \frac{\bar{k}}{J} & -\frac{\bar{k}}{J} & 0 & 0 \\ 0 & k_2 & -k_1 & 0 & k_3 & 0 \\ 0 & -k_2 & 0 & -k_1 & 0 & k_3 \\ k_3 c_3 \mu_1 k_p & -c_3 \mu_1 k_v & 0 & 0 & -c_1 & 0 \\ 0 & 0 & 0 & 0 & 0 & -c_1 \end{bmatrix}, \quad (36)$$

$$\mathbf{A}_2 = \begin{bmatrix} 0 & -1 & 0 & 0 & 0 & 0 \\ 0 & -\frac{F_v}{J} & \frac{\bar{k}}{J} & -\frac{\bar{k}}{J} & 0 & 0 \\ 0 & k_2 & -k_1 & 0 & k_3 & 0 \\ 0 & -k_2 & 0 & -k_1 & 0 & k_3 \\ 0 & 0 & 0 & 0 & -c_1 & 0 \\ -k_3 c_3 \mu_1 k_p & c_3 \mu_1 k_v & 0 & 0 & 0 & -c_1 \end{bmatrix}. \quad (37)$$

4.3 Experimental platform

In order to evaluate the performance of the studied controllers, we have carried out real-time experiments on a Pittman 14207S008 DC motor driven by a servo amplifier model 30A20AC from Advanced Motion Controls, which is configured in current mode. To execute real-time experiments the motor is controlled through a PC and a data acquisition board Sensoray 626, which is used to read the quadrature optical encoder signals and transfer the control signal to the servo amplifier. Fig. 8 shows a picture of the motor and Fig. 9 depicts a block diagram of the experimental system. Algorithms are executed at a sampling frequency of 1 kHz on Windows XP using Matlab with Simulink and the Real-Time Windows Target.



Fig. 8 DC motor Pittman 9236S009.

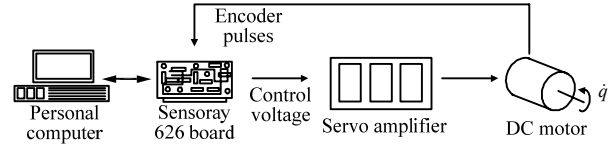


Fig. 9 Block diagram of the experimental system.

Velocity is obtained through Euler differentiation

$$\dot{q}(kT) = \frac{q(kT) - q((k-1)T)}{T},$$

where $k = 1, 2, 3, \dots, n$, is the discrete time and $T = 0.001$ s is the sampling period.

4.4 Tuning of the control gains and closed-loop stability

By using the necessary condition for asymptotical stability under arbitrary commutation, which requires that the individual subsystems should be stable^[23], the root locus method of the characteristic equation of the each subsystem $\dot{\mathbf{x}} = \mathbf{A}_i \mathbf{x}$, $i = 1, 2$, is used to compute the numerical values of the constants μ_1 , μ_2 , k_p and k_v such that \mathbf{A}_i , $i = 1, 2$ is a Hurwitz matrix.

Some previous experiments were carried out to obtain estimations of the motor parameters:

$$\begin{cases} \frac{F_v}{J} = 1.351, \\ \frac{\bar{k}}{J} = 5101. \end{cases} \quad (38)$$

The following parameters were selected for the musculotendon actuators:

$$\begin{cases} k_1 = k_3 = 700, \\ k_2 = 2, \\ c_1 = c_3 = 700, \\ c_2 = 0, \end{cases} \quad (39)$$

while in the switching control law the following numerical parameters

$$\begin{cases} \mu_1 = 1, k_p = 0.3, \\ \mu_2 = 1, k_v = 0.01, \end{cases} \quad (40)$$

were used. It is worthwhile to remark that the physical sense of the parameters Eq. (39) is obtained by comparing Eqs. (32) and (33). Thus, $k_1 = 30 F_{01}^M / L_{s1}^T$ and $k_3 = 30 F_{01}^M V_{m1} / L_{s1}^T$, while c_1 , c_2 and c_3 are the parameters of the activation dynamics Eq. (33). The numerical values of the musculotendon and switching control law parameters in Eqs. (39) and (40), respectively, guarantee

that the matrices Eqs. (36) and (37) are Hurwitz.

Next step is to show that the state space origin of the switched system Eq. (34) is locally asymptotically stable. To this aim, by using SOSTOOL, a numerical common Lyapunov function satisfying inequalities Eqs. (19) and (20) for the linearized system Eq. (35) has been computed. Specifically, such a common Lyapunov function is

$$V(\mathbf{x}) = \mathbf{x}^T \mathbf{P} \mathbf{x} \quad \mathbf{x} \in \mathbb{R}^6, \mathbf{P} = \mathbf{P}^T > 0, \mathbf{P} \in \mathbb{R}^{6 \times 6}, \quad (41)$$

$$\text{where } \mathbf{P} = \begin{bmatrix} p_{11} & p_{12} & p_{13} & p_{14} & p_{15} & p_{16} \\ p_{21} & p_{22} & p_{23} & p_{24} & p_{25} & p_{26} \\ p_{31} & p_{32} & p_{33} & p_{34} & p_{35} & p_{36} \\ p_{41} & p_{42} & p_{43} & p_{44} & p_{45} & p_{46} \\ p_{51} & p_{52} & p_{53} & p_{54} & p_{55} & p_{56} \\ p_{61} & p_{62} & p_{63} & p_{64} & p_{65} & p_{66} \end{bmatrix},$$

in which $p_{11} = 5142$, $p_{12} = p_{21} = -16.3665$, $p_{13} = p_{31} = -62.095$, $p_{14} = p_{41} = 62.095$, $p_{15} = p_{51} = -4.798$, $p_{16} = p_{61} = 4.798$, $p_{22} = 3.7663$, $p_{23} = p_{32} = 26.463$, $p_{24} = p_{42} = -26.463$, $p_{25} = p_{52} = 25.6495$, $p_{26} = p_{62} = -25.6495$, $p_{33} = p_{44} = 194.98$, $p_{34} = p_{43} = -192.855$, $p_{35} = p_{53} = p_{46} = p_{64} = 190.805$, $p_{36} = p_{63} = p_{45} = p_{54} = 189.795$, $p_{55} = p_{66} = 192.49$, $p_{56} = p_{65} = 189.655$.

The function Eq. (41) allows concluding, by Theorem 1, that the state space origin $\mathbf{x} = 0 \in \mathbb{R}^6$ of the switched system Eq. (35) is globally asymptotically stable. Then, by Theorem 2, that the state space origin $\mathbf{x} = 0 \in \mathbb{R}^6$ of the nonlinear switched system Eq. (34) is locally asymptotically stable.

4.5 Simulation and experimental results

The specified desired position is $x_d = 4$ rad. The initial conditions for the overall system are

$$\begin{bmatrix} \tilde{x}_1(0) \\ x_2(0) \\ x_3(0) \\ x_4(0) \\ x_5(0) \\ x_6(0) \end{bmatrix} = \begin{bmatrix} 4 \\ 0 \\ 0 \\ 0 \\ 0 \\ 0 \end{bmatrix}.$$

We show simulation and experimental results of the nonlinear system Eq. (33) using the nonlinear controller Eqs. (22) and (23). Fig. 10 shows the time evolution of the motor shaft position. The control inputs $u_1(t)$, $u_2(t) \in [0,1]$ to the musculotendon actuators 1 and 2 are presented in Fig. 11. The time history of the Lyapunov

function $V(\mathbf{x})$ in Eq. (41) has been computed for the switched nonlinear system Eq. (34) and the continuous lines to the switched linearized system Eq. (35). This result is shown in Fig. 12, where vertical lines indicate the commutation time of regions 1 and 2.

Let us notice that the initial position error $\tilde{x}(0) = 4$ rad is relatively high. However, thanks to the incorporation of the hyperbolic tangent function, which is a smooth and bounded function, the switched control signals Eqs. (22) and (23) remain bounded for all time, as seen in Fig. 11. As soon as the actual position $x_1(t)$ goes to the desired one x_d , the numerical values of the neural excitations $u_1(t)$ and $u_2(t)$ decrease and the closed-loop system becomes more stable. Finally, Fig. 13 shows the voltage applied to the motor, which also goes to zero as time increases.

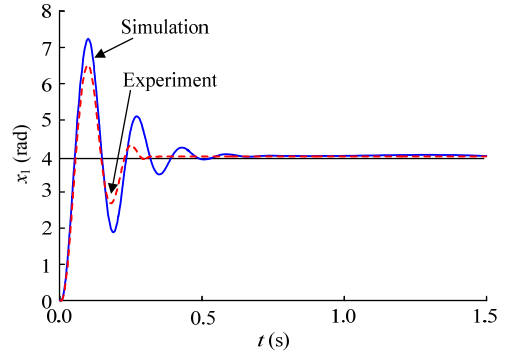


Fig. 10 Position error $x_1(t)$.

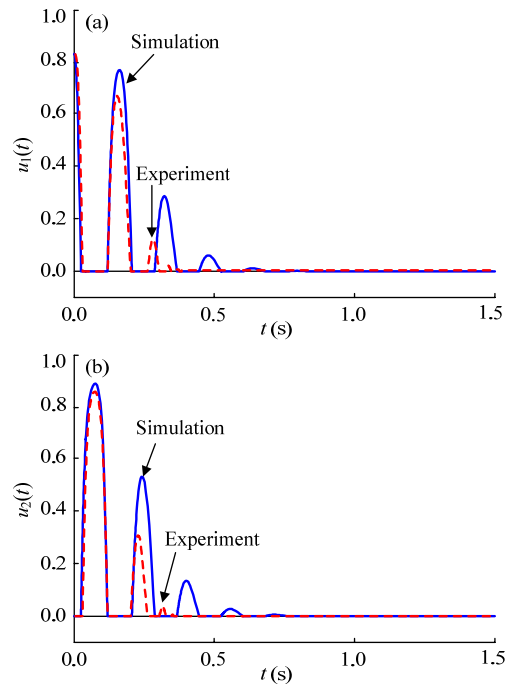


Fig. 11 Neural excitations $u_1(t)$ and $u_2(t)$ by simulation and experiment respectively.

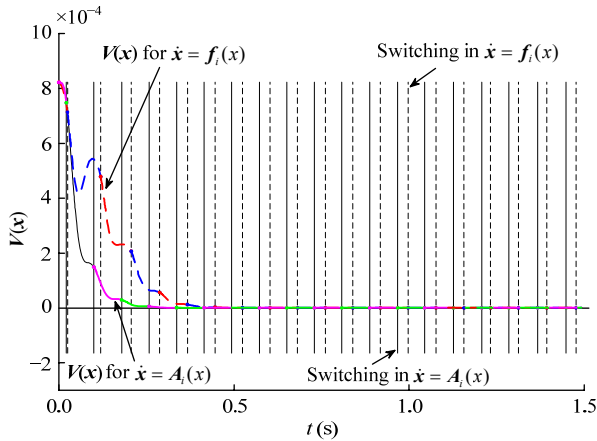


Fig. 12 Common Lyapunov function $V(x)$. The dashed lines correspond to the switched nonlinear system Eq. (34) and the continuous lines to the switched linearized system Eq. (35).

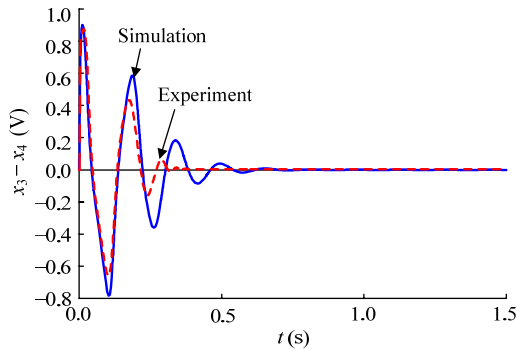


Fig. 13 Time history of the voltage applied to the motor $v(t) = x_3(t) - x_4(t)$ by simulation and experiment respectively.

5 Conclusions and further research

This work presented the modelling, control and simulation of a second order mechanical system actuated by two Zajac's musculotendon subsystems in an agonist-antagonist configuration. An important assumption was that the musculotendon subsystems have constrained neural excitation inputs $u_1(t), u_2(t) \in [0,1]$. The stability theory of switched systems, the root locus method for linear systems, and SOSTOOLS were used to design a saturated semi positive neural excitation inputs $u_1(t)$ and $u_2(t)$, which stabilize the studied biomechanical system. Finally, the application of the proposed ideas to a mechatronic system was introduced.

The main limitation of the proposed control approach is that it only uses information of the mass position and velocity of the mass, that is, the controller is based on partial state feedback. The feedback of the activation levels and applied forces could increase the performance of the motion, because the design based on root-locus of the linearized subsystems in Eq. (25)

would be easier thanks to the introduction of the more control gains. The incorporation of a state observer and the respective stability analysis is a topic that deserves study also.

Let us notice that the development of an extension of the proposed approach to the trajectory tracking control is still in study. However, simulations have shown that the introduced control scheme can guarantee uniform ultimate boundedness of the trajectory tracking error $\tilde{x}_i(t)$. Besides, the ultimate bound of the trajectory tracking error is inversely proportional to the values of the control gains. In other words, the greater the values of the gains, the lower the value of the ultimate bound. Notwithstanding, at this time the mathematical proof of this claim requires more refinement.

Another problem that has been considered as further research is the relationship of the proposed control approach with the actual control of a real human arm. In this respect, the proposed controller could be interpreted as a system for which identification of the control gains from electromyographic signals could be achieved, which would support the idea that the controller programmed in the human body belongs to the class of switched systems.

Acknowledgments

This work is partially supported by CONACyT and SIP-IPN, Mexico. The authors also wish to thanks Dr. F. Zajac for his valuable answers related to the musculotendon model and Dr. A. Papachristodoulou for his generous help with SOSTOOLS.

References

- [1] Zajac F E. Muscle and tendon: properties, models, scaling, and application to biomechanics and motor control. *Critical Reviews in Biomedical Engineering*, 1989, **17**, 359–411.
- [2] Hill A V. The heat of shortening and the dynamic constants of muscle. *Proceedings of the Royal Society of London B, Biological Sciences*, 1938, **126**, 136–195.
- [3] Huxley A F. Muscle structure and theories of contraction. *Progress in Biophysics and Biophysical Chemistry*, 1957, **7**, 255–318.
- [4] Epstein M, Herzog W. *Theoretical Models of Skeletal Muscle: Biological and Mathematical Considerations*, John Wiley & Sons, New York, 1998.
- [5] He J, Levine W S, Loeb G E. Feedback gains for correcting small perturbations to standing posture. *IEEE Transactions*

- on *Automatic Control*, 1991, **36**, 322–332.
- [6] Martin C F, Schovanec L. Muscle mechanics and dynamics of ocular motion. *Journal of Mathematical Systems, Estimation and Control*, 1998, **8**, 1–15.
- [7] Menegaldo L L. *Modelagem Biomecânica e Controle Ótimo da Postura Humana Através de Algoritmos Baseados na Teoria das Aproximações Consistentes*, PhD, Escola Politécnica da Universidade de São Paulo, Departamento de Engenharia Mecânica, São Paulo, 2001. (in Portuguese)
- [8] Farahat W, Herr H. Workloop energetics of antagonist muscles. *Proceedings of the 28th IEEE EMBS Annual International Conference*, New York, USA, 2006, 3640–3643.
- [9] Winters J M, Stark L. Muscle models: What is gained and what is lost by varying model complexity. *Biological Cybernetics*, 1987, **55**, 403–420.
- [10] Thelen D, Blemker S, Anderson C, Delp S. Dynamic Modeling and Simulation of Muscle-Tendon Actuators. Notes of the lecture ME 382: Modeling and Simulation of Human Movement, Stanford University, 2001.
- [11] Pandy M G, Zajac F E, Sim E, Levine W. An optimal control model for maximum-height human jumping. *Journal of Biomechanics*, 1990, **23**, 1185–1198.
- [12] Iqbal K, Roy A. Stabilizing PID controllers for a single-link biomechanical model with position, velocity, and force feedback. *Journal of Biomechanical Engineering*, 2004, **126**, 838–843.
- [13] Tahara K, Luo Z W, Arimoto S, Kino H. Sensory-motor control mechanism for reaching movements of a redundant musculo-skeletal arm. *Journal of Robotic Systems*, 2005, **22**, 639–651.
- [14] Moody C B, Barhorst A A, Schovanec L. A neuro-muscular elasto-dynamic model of the human arm part 2: Musculotendon dynamics and related stress effects. *Journal of Bionic Engineering*, 2009, **6**, 108–119.
- [15] Laczko J, Pilišsy T, Tibold R. Neuro-mechanical modeling and controlling of human limb movements of spinal cord injured patients. *Proceedings of the 2nd International Symposium on Applied Sciences in Biomedical and Communication Technologies*, Bratislava, Slovakia, 2009, 1–2.
- [16] Liberzon D. *Switching in System and Control*, Birkhäuser, Boston, USA, 2003.
- [17] Beldiman O, Bushnell L. Stability, linearization and control of switched systems. *Proceedings of the American Control Conference*, San Diego, USA, 1999, 2950–2954.
- [18] Prajna S, Papachristodoulou A. Analysis of switched and hybrid systems-beyond piecewise quadratic methods. *Proceedings of the 2003 American Control Conference*, Denver, USA, 2003, 2779–2784.
- [19] Papachristodoulou A, Prajna S. A tutorial on sum of squares techniques for systems analysis. *Proceedings of the 2005 American Control Conference*, Portland, USA, 2005, 2686–2700.
- [20] Prajna S, Papachristodoulou A, Seiler P, Parrilo P A. *SOSTOOLS: Sum of Squares Optimization Toolbox for MATLAB*, [2004-06-01], <http://www.mit.edu/parrilo/sostools>
- [21] Bar-Cohen Y, *Biomimetics: Biologically Inspired Technologies*, CRC Press, Boca Raton, 2006.
- [22] Gottlieb G L, Agarwal G C. Dynamic relationship between isometric muscles tension and the electromyogram in man. *Journal of Applied Physiology*, 1971, **30**, 345–351.
- [23] Liberzon D, Morse S. Basic problems in stability and design of switched systems. *IEEE Control Systems Magazine*, 1999, **19**, 59–70.
- [24] Cavallaro E E, Rosen J, Perry J C, Burns S. Real-time myoprocessors for a neural controlled powered exoskeleton arm. *IEEE Transactions on Biomedical Engineering*, 2006, **53**, 2387–2396.
- [25] Baratta R, Solomonow M, Zhou B H, Letson D, Chuinard R, D'Ambrosia R. Muscular Coactivation. The role of the antagonist musculature in maintaining knee stability. *American Journal of Sports Medicine*, 1988, **16**, 113–122.
- [26] Solomonow M, Baratta R, Zhou B H, D'Ambrosia R. Electromyogram coactivation patterns of the elbow antagonist muscles during slow isokinetic movement. *Experimental Neurology*, 1988, **100**, 470–477.
- [27] Tsuji T, Tanaka Y, Morasso P, Sanguineti V, Kaneko M. Bio-mimetic trajectory generation of robots via artificial potential field with time base generator. *IEEE Transactions on Systems, Man, and Cybernetic Part C: Applications, and Reviews*, 2002, **32**, 403–420.
- [28] Hashimoto S, Narita S, Kasahara H, Takanishi A, Sugano S, Shirai H, Kobayashi T, Takanobu H, Kurata T, Fujiwara K, Matsuno T, Kawasaki T, Hoashi K. Humanoid robot-development of an information assistant robot hadaly. *Proceedings of the 8th IEEE International Workshop on Robot and Human Communication*, Pisa, Italy, 1997, 106–111.
- [29] Hirai K, Hirose M, Haikawa Y, Takenaka T. The development of honda humanoid robot. *Proceedings of the 1998 IEEE International Conference on Robotics and Automation*, Leuven, Belgium, 1998, 1321–1326.